Chemistry of the Total Environment 2023, 3(1): 1-7

GLINTPLUS

ISSN: 2805-3419

Research Article

An efficient photo reactor design and its application in photo-oxidation of acetone

Emmanuel A. Kamba*, Daniel I. Ugwuja, Emmanuel A. Yerima and Godwin O. Egah

Chemical Sciences Department, Faculty of Pure and Applied Sciences, Federal University Wukari. PMB 1020, Taraba State, Nigeria

ABSTRACT

The rate of CO_2 production obtained from the photodecomposition of acetone with different loadings of TiO_2 as a photocatalyst is remarkable. This study aims to develop a flow-type photo reactor with excellent contact between all the reacting species. To achieve total mineralization with minimal waste, the flow rate of gases was controlled. During this investigation, the acetone was fed at the rate of 2.8 mmol h^{-1} and the air flow rate was maintained at 4.3 Lh^{-1}. The reaction was carried out at near room temperature as the cold cathode lamps increased temperature very slowly to 63 °C. No CO_2 was produced either without light or catalyst indicating a photocatalytic reaction. There was a proportional increase in the production of CO_2 with an increase in TiO_2 loading. A maximum rate of 5.75 ± 0.07 mMh^{-1} for CO_2 production was achieved with a catalyst loading of 5 mg/g_{beads}. Increasing the catalyst loading above 5 mg/g showed a decrease in CO_2 production rate which can be attributed to reduced contact between light and catalyst. This technique used here can be adopted for the decomposition of various Volatile Organic Compounds (VOCs).

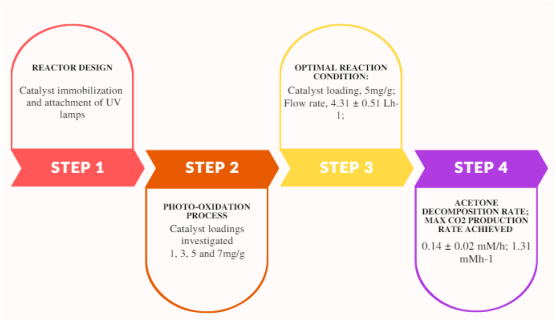

HIGHLIGHTS

- A new catalyst immobilization technique was investigated.
- A transparent glass beads were used for the reactor for excellent UV exposure.
- No CO_2 was observed in the absence of light, catalyst or oxidant.
- The formation of CO_2 from adsorbed carbonaceous is possible.

Article History:
Received: 27th June, 2022
Revised: 19th July, 2022
Accepted: 24th December, 2022
Available online: 1st May, 2023

Keywords:
Acetone; photoreactor; photooxidation; photodecomposition

1. Introduction

For a photocatalytic reaction, simultaneous contact between the reactants, catalyst and light (photons) is necessary. To minimise the e^-/h^+ recombination rate, the catalyst particles must be sufficiently small (tens of nanometres) (Liu et al., 2012) which renders conventional mechanical filtration ineffective. Certain coupled catalysts such as Fe_3O_4-TiO_2 core-shell however, can be separated from the reaction mixture using magnetic separation. This type of reactor is used for wastewater treatment, especially where post-reaction purification can be carried out easily. For gas phase reaction applications, it is possible to monitor reactions spectroscopically as they proceed in situ (El-Maazawi *et al*., 2000; He *et al*., 2013; Li *et al*., 2016; Liu *et al*., 2012; Song *et al*., 2015). However, the catalysts must be immobilised to achieve homogeneous illumination. Meanwhile, the supporting medium needs to be transparent to avoid light absorption and blocking by the solid substrates. The chemical reactants and products can be effectively separated from the immobilised catalysts which are essential for a flow reactor (Li *et al*., 2011).

Several types of photo-reactors have been created and used in the literature. Some of which include closed static reactors for gaseous reactants and solid catalyst which is either used as a free powder or immobilised on some supports such as quartz, (Fraters, 2015) wool, (De Lasa et al., 2005) mesh (Li *et al*., 2011) etc. However, the light illumination in such photoreactors is less homogeneous. To overcome this problem, photo-reactors with powdered catalysts suspended in a suitable solvent to form a slurry or (usually) coated on the walls of the reactor tube have been developed (Horie *et al*., 2010; Krishnan & Swaminathan, 2010). In such situations, the light illumination is improved, but the contact between the gaseous reactants and catalysts is significantly reduced.

Photoreactions have also been reportedly performed in a continuous flow system in which the catalyst is immobilised on

* CONTACT: E. A. Kamba; eacambah@gmail.com; Chemical Sciences Department, Federal University Wukari. PMB 1020, Taraba State. Nigeria
https://doi.org/10.52493/j.cote.2023.1.57

several materials such as glass rods (Li *et al*., 2011), mesh (Henderson, 2008), sponge (Lin et al., 2013), silica gel (Verbruggen *et al*., 2012) and a lot more, to maximise the contact between reactants and catalysts without sacrificing the light illumination (Fujishima *et al*., 2000).

Since the concentration of gaseous pollutants is typically low (in order of 10^{-9} M) (Raillard et al., 2004; Nagda & Rector, 2003) diffusion-limitations of reactions,(Fujishima *et al*., 2000) are not an issue for most domestic applications. Interestingly, using an adsorbent catalyst support can improve the performance of the photoreactor as the adsorbent support can increase the concentration of substrate near the catalyst relative to the gas-phase. This acts as a storage for the reactants that can diffuse to available active sites on catalyst while preventing the escape of reaction intermediates and driving the reaction to completion. This suggests that choice of support can influence the rates of adsorption, surface diffusion as well as desorption (Nagda & Rector, 2003).

For a functional flow reactor, immobilisation of the catalyst is required. There are several advantages associated with this procedure. The main advantage is that the catalyst/product separation problem can be circumvented. Different ratios of products could be obtained by simply tuning the flow rate/contact time and it is possible to operate continuously. This type of reactor can be considered suitable for industrial applications for both liquid and gaseous samples. Nevertheless, in gas-phase systems, the catalyst/substrate contact area is reduced which is a drawback, although the light illumination is maximized (Fujishima *et al*., 2008). Loss of catalyst and deactivation due to accumulation of less reactive intermediates are also possible issues (Henderson, 2008; Fujishima et al., 2008). In this work-type photo reactor was constructed and tested for photodecomposition of acetone in gas-phase. Flow reactors with immobilised catalysts have been reported to perform optimally for gas-phase photoreactions (Verbruggen et al., 2012; Nguyen et al., 2015). However, efficiency can be achieved by careful design as well as the selection of some reactor parameters which include the source of UV light, reactor configuration, lamp location, type of catalyst, distribution and impregnation of catalyst and more importantly, the interaction between the light, catalyst and reacting substrate (Henderson *et al*., 2008). The main objective of this study is to develop a flow-type photo reactor that can achieve high efficiency by providing excellent contact between the reacting species. As such controlled flow rates of gases were key to achieving total mineralization of acetone with minimal wastes. The gas phase reactor used in this work is highly compatible with photocatalytic reactions since the light can illuminate the whole reaction vessel uniformly. This feature can be of high industrial importance, especially in the area of the manufacture of air-cleaning devices.

2.0 Materials and Methods

2.1 Construction of photo-reactor

The reactor used in this work was similar to that of Verbruggen *et al*. (2011) but modified to enhance its efficiency. This was achieved by the addition of extra lamps which were attached to the outside walls of the reactor tube. The final reactor design (Figure 1), consisted of a quartz tube (400 mm length, 24/28 mm internal/external diameter) surrounded with 8 cold-cathode fluorescent UV_A lamps (wavelength 365.44 nm) each being; 305 mm length and 4.0 mm diameter. Another lamp was placed in the centre of the reactor tube making it 9 lamps each having a peak intensity of 22.6 mW power output. The reactor was filled with glass beads coated with a catalyst. Both ends of the reactor were sealed with rubber bungs which were pre-installed with steel tubing (6 mm external diameter) plugged with quartz wool, to give an appropriate gas inlet/outlet. All connections were sealed with epoxy glue for achieving airtight connections. Aluminium foil was

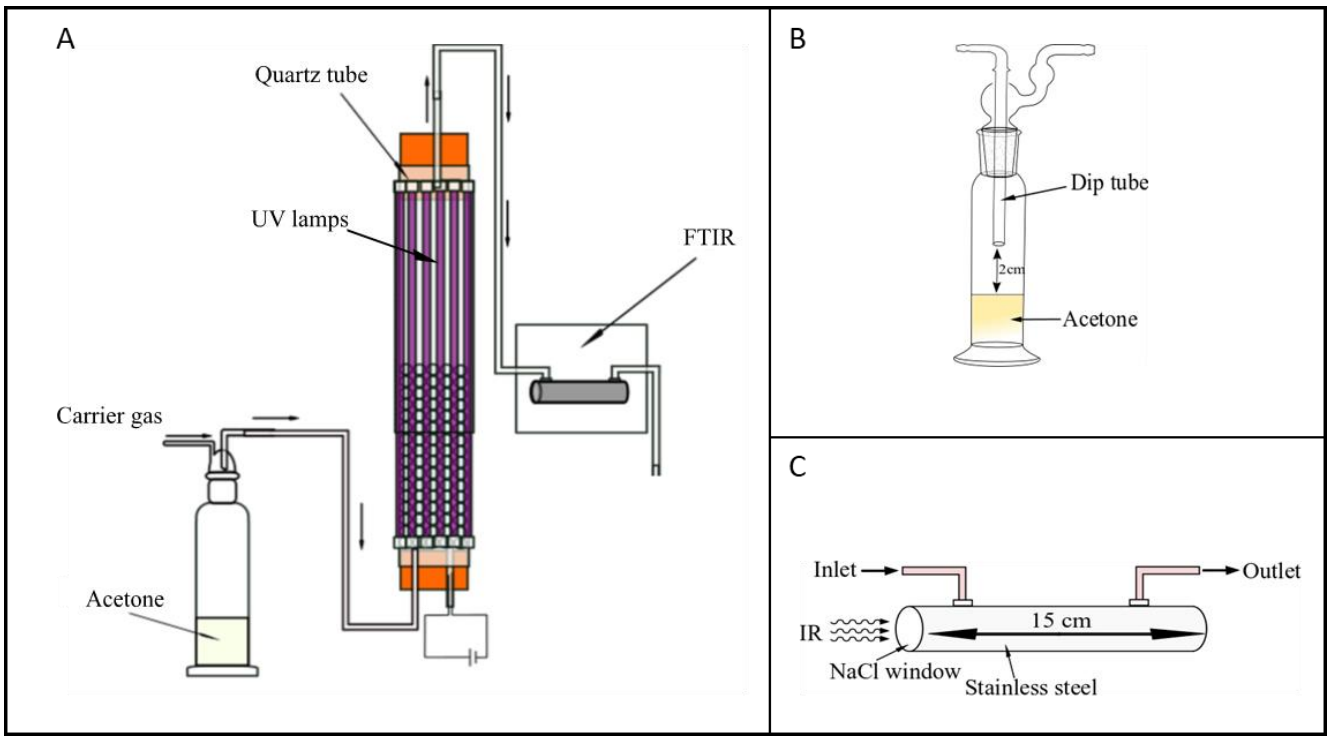

Figure 1: (A) Schematic diagram showing the experimental set-up, (B) the setup for the Dreschel bottle and (C) FTIR sampling cell.

then wrapped around the reactor to avoid the escape of UV radiation. The dead reactor volume was calculated to be approximately 56 cm^3.

2.2 Catalyst immobilisation

Prior to pre-treatment, the glass beads were washed with acetone and then refluxed for 2 hours in 6M NaOH. The glass beads were rinsed with deionised water until the washings were neutral, then rinsed with ethanol and allowed to dry in the air. This was followed by weighing to account for any loss in mass that could have resulted from the base treatment. The glass beads were then coated overnight with appropriate amounts of catalyst (TiO_2) to give loadings of 1-7 $mg_{catalyst}/g_{beads}$, followed by a second weighing to check the catalyst loading.

2.3 Introduction of acetone in the gas stream

Following a modified procedure reported by Lin *et al*., (2013) 5 ml of acetone in liquid form was placed in a Dreschel bottle under a continuous gas stream. Using compressed air as carrier gas at a flow rate of 4.31 ± 0.51 L/h, acetone was introduced to the reactor.

Due to the high volatility of acetone, the inlet concentration was controlled by maintaining the dip tube in the Dreschel bottle at 2 cm above the liquid to diffuse the acetone vapour, shown in Figure 1B. The vapour was collected by the outlet tube on the top. In this arrangement, if the dip tube is moved closer to the liquid level, the acetone vapour concentration will increase and vice versa. If the dip tube is below the liquid level, the concentration of acetone in the mix will be too high for the photoreactor and detection. The true concentration of acetone introduced in the flow reactor was measured by FTIR where the gas stream was passed through a gas sampling cell mounted in the optical pathway of the FTIR (Figure 1A). The length of the sampling stainless steel tube is fixed at 15 cm. Either NaCl, KBr or CaF_2 discs were used as IR windows, (see Figure 1C). After balancing the adsorption equilibrium by the photoreactor and catalysts in the dark, the lights were turned on and the acetone and CO_2 concentrations were monitored. By monitoring these concentrations, it was possible to gain insight into the photo-degradation kinetics of acetone by TiO_2 photocatalysts, thus confirming the functionality of the designed reactor.

3.0 Results and Discussion

3.1 Effectiveness of acetone photo-degradation

For environmental treatment, VOCs have to be mineralized into CO_2 and H_2O without a trace of organic fragments. Otherwise, such fragments might cause more hazards than the original VOCs. By applying UV illumination on the photoreactor fed with acetone and air, CO_2 gas was increased immediately. The transient plot for the CO_2 concentration with the light on and off is shown in Figure 2.

Verbruggen *et al.* (2011) reported a similar increase in CO_2 concentration in their study of the photodecomposition of acetone. When the light is switched on, the initial concentration slowly increased to the saturation concentration, while the gas flow is constant. This suggests that the created CO_2 might be adsorbed by the catalysts until the surface is saturated. By increasing the reaction temperature, the adsorption can be reduced and one might expect a faster increase in the CO_2 concentration. It is worth mentioning that no CO_2 was observed in the absence of either light or catalyst. Hence it confirms the nature of the photocatalytic mechanism (Scheme 1).

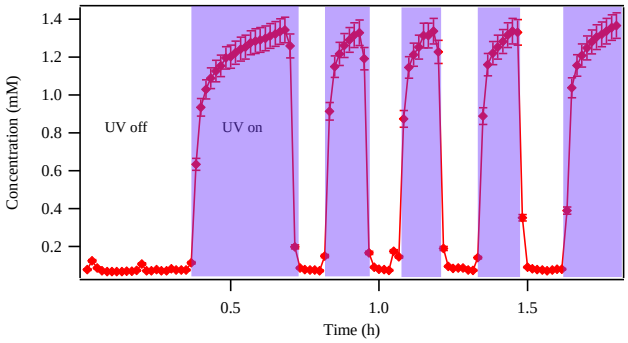

Figure 2. Concentration of CO_2 in a gas stream containing acetone versus flow time with the UV illumination on and off.

The sharp drop of CO_2 concentration when the light was switched off possibly reflects the decaying kinetics of the excited states in TiO_2 and the desorption kinetics of the adsorbed CO_2. As the desorption is normally slower, hence the decrease of CO_2 when light is off is dominated by the slow desorption kinetics alone. As it has been established that the concentration of CO_2 in the gas stream is due to the complete mineralization of acetone by TiO_2 photocatalyst, it became necessary to evaluate the effect of catalyst loading on the glass beads by monitoring the increase in CO_2 concentration per load. This is the focus of the next section.

3.2 Effects of catalyst loading

The amount of catalysts loaded on each beads could affect the photocatalytic reaction rate. At lower loading, there was not enough TiO_2 particles to be excited and to contact acetone, so the overall reaction rate will be low. At higher loading, each bead will absorb more photons and will result in insufficient, un-uniform light illumination. As a result, the reaction rate will also be reduced. Hence an optimum catalyst loading exists which balances the light illumination and contact with reactants. To find the optimum loading, the reaction rate was measured as a function of TiO_2 loading.

Here the reaction rate is defined by the CO_2 eluting rate, r_{CO_2}, at constant gas flow and constant light illumination. The CO_2 production rate, r_{CO_2}, was calculated as the product of the gas flow rate, *f*, and the CO_2 concentration, [CO_2], shown in Equation (1). The CO_2 concentration was determined by the FTIR signal intensity at 2300 cm^{-1} calibrated with known CO_2 concentration.

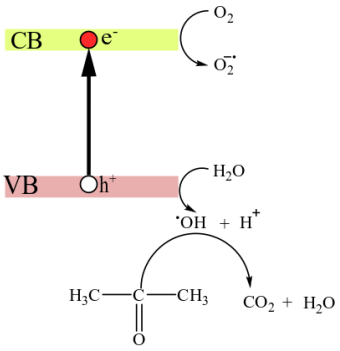

Scheme 1: Mechanism for the photocatalytic decomposition of acetone

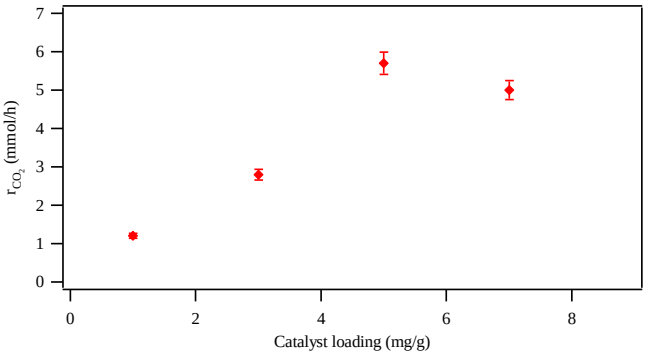

Figure 3. CO_2 production rates from the photodecomposition of acetone at different catalyst loading.

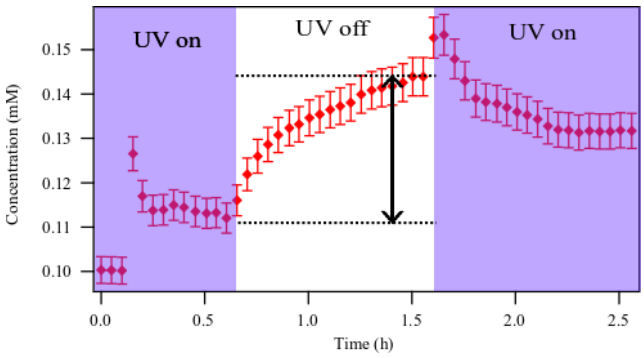

Figure 4. Acetone concentration in the presence and absence of UV illumination using 5 mg/g catalysts. The initial acetone concentration was regarded as the background and has been subtracted. The difference between the two steady-state concentrations used to determine the decomposition rate of acetone is shown by the dotted lines and arrow.

The intensity of the CO_2 under dark conditions was also subtracted. A similar method was used for measuring the acetone flow rate. By considering the contributions of gas flow rate to the concentration, the flow rate of CO_2 makes a better representation of CO_2 production in comparison with the molar concentration, since the molar concentration can be affected by the overall gas flow rate, hence the reason for this approach.

$$r_{CO_2} = f[CO_2] \qquad Equation\ 1$$

The rate of CO_2 production obtained from the photodecomposition of acetone with different loadings of TiO_2 is presented in Figure 3. During this measurement, the acetone was fed at the rate of 2.8 mmol/hr and the airflow rate is maintained at 4.3 L/h. The reaction was carried out at near room temperature as the cold cathode lamps increase temperature very slowly to 63 °C.

As shown here, there was a proportional increase in the production of CO_2 with the increase in TiO_2 loading. This observed increase in CO_2 production continued until a maximum rate of 5.75 ± 0.07 mM_{CO_2}/ h was achieved with a catalyst loading of 5 mg/g_{beads}. Loading greater than 5 mg/g showed a decrease in CO_2 production rate which can be attributed to reduced light/catalyst contact. In this case, only catalyst closest to the light source became activated as the coating was too thick. Excess catalyst loading resulted in enhanced local UV adsorption and potentially, increased the surface area as well as active sites for the photocatalytic decomposition of acetone. An optimum catalyst loading of 5 $mg/g_{beads}$was found to be the best TiO_2 loading for maximum efficiency of photodecomposition of acetone under the studied conditions.

3.3 Decomposition of acetone

To study the photodecomposition process of acetone, the flow rate of acetone with and without light was monitored. As can be seen in Figure 4, upon UV illumination, a rapid initial increase in the concentration of acetone was observed until a steady state was reached; during which the acetone adsorption and decomposition were balanced on the catalyst surface. When the UV irradiation was turned off, the photodecomposition process became halted which resulted in a slow rise in the concentration of acetone until another steady state was reached. The increase in acetone concentration at the beginning of the light cycle, followed by a gradual increase after the light is turned off, suggests that adsorption has a significant effect. The illumination of light causes the desorption of acetone, and when the light is turned off, the acetone in the feed is adsorbed back onto the catalyst surface.

The actual concentration of photodecomposed acetone [A], is given by the difference between the concentrations in dark and under illumination, $[A]_{dark} - [A]_{UV}$. Knowing the gas flow rate, *f*, allows the determination of the rate of decomposition of acetone, $-r_A$using Equation 2. In this study, the gas flow rate was 4.3 mM/h and $[A]_{dark}$ is 0.145 mM while $[A]_{UV}$ is 0.113 mM, reading from Figure 4. Thus the acetone decomposition rate is 0.14 ± 0.02 mM/h.

$$-r_A = f([A]_{dark} - [A]_{UV}) \qquad Equation\ 2$$

The decomposition efficiency can also be characterised using the concept of conversion. Conversion is defined by the ratio between the decomposed acetone [*A*] and the inlet concentration $[A]_{dark}$ using Equation 3. In the present work conversion of 22 % was achieved for the photodecomposition of acetone, based on the values of $[A]_{dark}$ and $[A]_{UV}$ from Figure 4.

$$Conversion\ \% = \frac{[A]_{dark} - [A]_{UV}}{[A]_{dark}} \qquad Equation\ 3$$

A higher conversion value has been reported for the photodecomposition of acetone. Han *et al*., (2012) reported a 35% conversion of acetone in their study on the photodecomposition of acetone in gas-phase over Degussa P25. They attributed the higher conversion rate to their TiO_2 immobilisation substrate (polystyrene mesh) which allowed for a significant increase in gas-catalyst contact area for the glass beads used in the present study. However, the ease of handling the catalyst makes the immobilization technique used in this work a more industrially viable choice.

The photocatalytic mineralisation of acetone to CO_2 is known to proceed through various stable chemical intermediates and the mechanism largely depends on the experimental conditions. Several routes have been proposed in the literature for the photoconversion of acetone, many of which show that acetone undergoes several chemical transformations before finally mineralizing completely (El-Maazawi *et al*., 2000). However, there is a likelihood that many partial oxidation products were formed considering that during the photodecomposition of acetone, the initial oxidation steps are more kinetically favoured rather than total mineralization. (Henderson, 2008; Fujishima et al., 2008; Verbruggen et al., 2011) The partial oxidation products include

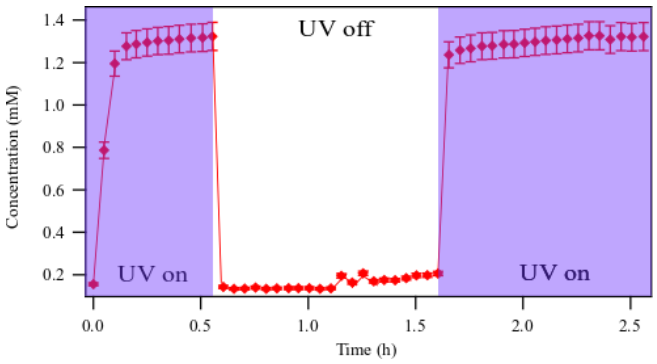

Figure 5: CO_2 concentration from acetone decomposition with and without UV illumination during the photodecomposition process

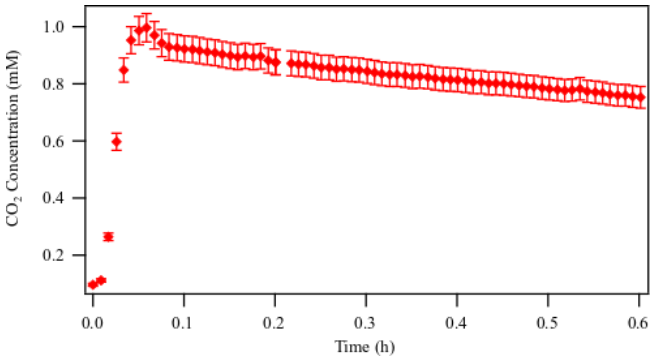

Figure 7: CO_2 concentration developed during the photocatalytic decomposition of carbonaceous residues on the TiO_2 under UV illumination with a clean gas in a flow

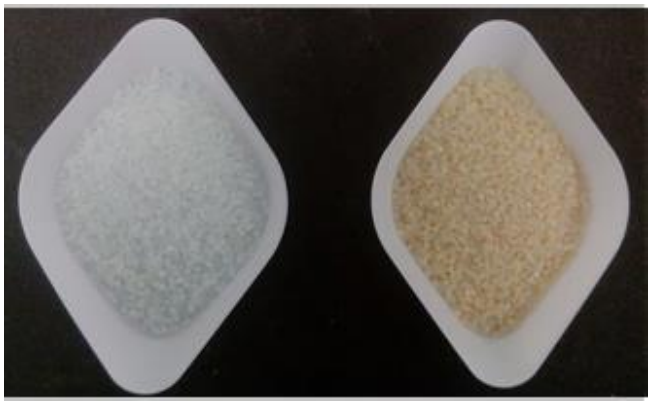

Figure 6: TiO_2 coated glass beads before (left) and after (right) photodecomposition reaction of acetone. Yellowish discoloration is due to accumulated carbonaceous species on TiO_2 surface.

many carbonyl moieties such as acetic acid, (Henderson, 2008; Sakai et al., 2013) formic acid, (Xu & Raftery, 2001) and mesityl oxide (El-Maazawi et al., 2000; Coronado et al.,, 2003; Xu & Raftery, 2001). Most of them are easily oxidized. In this experiment, variation in CO_2 produced was also monitored as shown in Figure 5. The maximum production rate of CO_2 was found to be 1.31± mM/h. This makes it 9.4 times as much as the corresponding decomposition rate of acetone (0.14 ± 0.02 mM/h).

Due to the stoichiometric ratio (1:3) between acetone and CO_2, it would be expected that the CO_2 concentration would only be 3 times of decomposed acetone. The higher-than-expected CO_2 concentration suggests there are other factors affecting the CO_2 concentration. The possible reason for this is that there are a significant amount of organic species, including acetone, and its partial oxidation products such as acetic acid, (Henderson, 2008; Sakai et al., 2013) formic acid, (Xu & Raftery, 2001) and mesityl oxide (El-Maazawi et al., 2000; Coronado et al., 2003; Xu & Raftery, 2001) were absorbed in the photoreactor. They are then gradually released after being oxidized into CO_2 since the reaction was carried out at room temperature. The adsorption behaviour was confirmed with the initial increase in the acetone concentration when the light was switched on. At room temperature, such adsorption is inevitable. As such, the parameter of conversion could underestimate the performance of the TiO_2 photoreactor. A high temperature measurement could eliminate the adsorption and could give a more accurate result.

The existence of intermediates could interfere with the measuring of acetone concentration. The extinction coefficient of these species will not be the same as that of acetone, consequently, the carbonyl peak area can increase by unknown amounts due to the contribution of the intermediates. As such, the observed reduction in the concentration of acetone could be overestimated.

Verbruggen *et al.* (2011) reported similar results where concentrations of produced CO_2 exceeded the complete mineralisation of the photo-decomposed species. They also suggested that the deposition of organic residue on the photocatalyst surface may be responsible for the high concentration of CO_2.

Further experiments were performed to investigate the extent of carbonaceous deposition on the surface of the catalyst. The amount of CO_2 output was measured under UV illumination without the input of acetone immediately after the decomposition of acetone. It can be seen in Figure 6 that by the switch on of the UV light, the concentration of CO_2 rose rapidly despite the absence of acetone in the system. This observed CO_2 formation must have resulted from the oxidation of adsorbed carbonaceous species. After reaching its peak at 3.5 min, the concentration of CO_2 decreases slowly as the adsorbed carbonaceous species became depleted. The maximum production rate of CO_2 was measured to be 0.90 ± 0.09 mM/h.

Having realised that CO_2 production is contributed by the decomposition of supplied acetone and the adsorbed organic species, it is possible to evaluate the net contribution of CO_2 production from the decomposition of acetone. From Figure 5, the maximum CO_2 production rate is about 1.31 mM/h. This value is reduced to 0.90 mM/h without acetone, in Figure 6. Hence, the net contribution to CO_2 production from acetone decomposition is 0.41 mM/h (1.31 mM/h-0.90 mM/h). From Figure 4, the acetone decomposition rate was found to be 0.14 mM/h. In comparison with the CO_2 production rate of 0.41 mM/h, the stoichiometric ratio of 3 for CO_2 vs acetone is almost satisfied. Thus, it is much more accurate to calculate the conversion directly from the acetone concentrations. However, it is difficult to get meaningful kinetic data from the CO_2 production rate, since it is distorted by the adsorption. This also confirms that the excess amount of CO_2 produced during the photodecomposition reaction of acetone can be ascribed to the decomposition of accumulated carbonaceous species on the catalyst surface together with the decomposition of acetone. Extended photodecomposition of acetone beyond 20 h also provided evidence of carbon deposition resulting in discolouration of TiO_2 catalyst-coated glass beads, shown in Figure 7.

Irrespective of the complexity associated with quantifying photocatalytic decomposition of acetone, it is comforting to know

that a successful photodecomposition at a constant rate of 0.14 ± 0.02 mM/h was achieved during this work. Interestingly, this value far outweighs the concentrations of acetone within domestic environments (2.2 - 9.9 nM). (Raillard et al., 2004; Nagda & Rector, 2003) Therefore, the photo-reactor so developed in this work can serve as a potential ambient air acetone removal system.

4.0 Conclusions

In this study, a new catalyst immobilization technique with high catalyst-support adherence efficiency has been demonstrated. The key equations used for the design of the photoreactor were derived. The reactor was designed to achieve a uniform irradiation field that affords plausible control over the average light intensity. The success of the design will produce more reliable experimental data and provide a more simplified photocatalytic process. A promising industrial implication is envisaged when an excellent catalyst adherence on the glass beads with high stability was achieved with the lowest catalyst loading amount. In this study, the gas-phase, flow-type photo-reactor was successfully tested for photodecomposition of acetone. The immobilisation method developed in this study is indeed complementary and simple to implement. By utilising a highly active, inexpensive commercially available photocatalyst (P25) it was possible to achieve acetone decomposition. The streamlined design of the reactor made it possible for all the reacting species to be in contact while the transparency of the glass beads provided an excellent UV light penetration to even the innermost part of the reactor, hence the observed high photo activity. The formation of CO_2 from carbonaceous species adsorbed on the surface of the catalyst during the photodecomposition reactions has been observed. Prolonged illumination in the absence of the reactant (acetone) can easily deplete the deposition of these accumulated carbonaceous species and release more active sites for the adsorption of the substrate. Since records have shown that the levels of indoor acetone pollution are typically in orders of magnitude lower than the concentrations used in this chapter, the designed reactor can therefore be a plausible initial step for the development of air purification devices.

CRediT authorship contribution statement

E. A. Kamba: Conceptualization, Methodology, Writing - original draft, Software, Data curation. D. I. Ugwuja: Methodology, Writing - original draft, Software, Writing - review & editing. E. A. Yerima: Methodology, Writing - review & editing. G. O. Egah: Data curation, Writing - review & editing, Resources.

Declaration of competing interest

The authors declare that they have no known competing financial interests or personal relationships that could have appeared to influence the work reported in this paper.

Acknowledgement

The authors appreciate Dr. Qiao Chen of Department of Chemistry, School of Life Sciences, University of Sussex, UK for granting us access to his laboratory.

Funding

This study was completely financed by the authors.

References

Coronado, J. M., Kataoka, S., Tejedor-Tejedor, I., & Anderson, M. A. (2003). Dynamic phenomena during the photocatalytic oxidation of ethanol and acetone over nanocrystalline TiO_2: Simultaneous FTIR analysis of gas and surface species. *Journal of Catalysis*, *219*(1), 219–230. https://doi.org/10.1016/S0021-9517(03)00199-4

De Lasa, H., Serrano, B., & Salaices, M. (2005). Photocatalytic reaction engineering. *Photocatalytic Reaction Engineering*. New York. https://doi.org/10.1007/0-387-27591-6

El-Maazawi, M., Finken, A. N., Nair, A. B., & Grassian, V. H. (2000). Adsorption and photocatalytic oxidation of acetone on TiO_2: An in situ transmission FT-IR study. *Journal of Catalysis*, *191*(1), 138–146. https://doi.org/10.1006/jcat.1999.2794

Fraters, B. D. (2015). *TiO_2 based photocatalytic gas purification; the effects of co-catalysts and process conditions*. Gildeprint drukkerijen, Enschede, The Netherlands. https://doi.org/10.3990/1.9789036538862

Fujishima, A., Rao, T. N., & Tryk, D. A. (2000). Titanium dioxide photocatalysis. *Journal of Photochemistry and Photobiology C: Photochemistry Reviews*, *1*(1), 1–21. https://doi.org/10.1016/S1389-5567(00)00002-2

Fujishima, A., Zhang, X., & Tryk, D. A. (2008). TiO_2 photocatalysis and related surface phenomena. *Surface Science Reports*. https://doi.org/10.1016/j.surfrep.2008.10.001

Han, Z., Chang, V. W. C., Zhang, L., Tse, M. S., Tan, O. K., & Hildemann, L. M. (2012). Preparation of TiO_2-Coated Polyester Fiber Filter by Spray-Coating and Its Photocatalytic Degradation of Gaseous Formaldehyde. *Aerosol and Air Quality Research*, *12*(6), 1327–1335. https://doi.org/10.4209/aaqr.2012.05.0114

He, J., Zhai, Q., Zhang, Q., Deng, W., & Wang, Y. (2013). Active site and reaction mechanism for the epoxidation of propylene by oxygen over CuOx/SiO2 catalysts with and without Cs+ modification. *Journal of Catalysis*, *299*, 53–66. https://doi.org/10.1016/j.jcat.2012.11.032

Henderson, M. A. (2008). Effect of coadsorbed water on the photodecomposition of acetone on TiO_2 (110). *Journal of Catalysis*, *256*, 287–292. https://doi.org/10.1016/j.jcat.2008.03.020

Horie, T., Sumino, M., Tanaka, T., Matsushita, Y., Ichimura, T., & Yoshida, J. I. (2010). Photodimerization of maleic anhydride in a microreactor without clogging. *Organic Process Research and Development*, *14*(2), 405–410. https://doi.org/10.1021/op900306z

Krishnan, J., & Swaminathan, T. (2010). Kinetic modeling of a photocatalytic reactor designed for removal of gas-phase benzene: A study on limiting resistances using design of experiments. *Latin American Applied Research*, *40*(4), 359–364.

Li, T., Zeng, W., Long, H., & Wang, Z. (2016). Nanosheet-assembled hierarchical SnO2 nanostructures for efficient gas-sensing applications. *Sensors and Actuators, B: Chemical*, *231*, 120–128. https://doi.org/10.1016/j.snb.2016.03.003

Li, Y., Yu, H., Song, W., Li, G., Yi, B., & Shao, Z. (2011). A novel photoelectrochemical cell with self-organized TiO_2 nanotubes as photoanodes for hydrogen generation. *International Journal of Hydrogen Energy*, *36*(22), 14374–14380. https://doi.org/10.1016/j.ijhydene.2011.08.026

Lin, L., Chai, Y., Zhao, B., Wei, W., He, D., He, B., & Tang, Q. (2013). Photocatalytic oxidation for degradation of VOCs. *Open Journal of Inorganic Chemistry*, *03*(01), 14–25. https://doi.org/10.4236/ojic.2013.31003

Liu, L., Zhao, H., Andino, J. M., & Li, Y. (2012). Photocatalytic CO_2 Reduction with H_2O on TiO 2 Nanocrystals: Comparison of Anatase, Rutile, and Brookite Polymorphs and Exploration of Surface Chemistry. *ACS Catalysis*, *2*(8), 1817–1828. https://doi.org/10.1021/cs300273q

Nagda, N. L., & Rector, H. E. (2003). A critical review of reported air concentrations of organic compounds in aircraft cabins. *Indoor Air*, *13*(3), 292–301. https://doi.org/10.1034/j.1600-0668.2003.00202.x

Nguyen, V.-H., Lin, S. D., Wu, J. C. S., & Bai, H. (2015). Influence of co-feeds additive on the photo-epoxidation of propylene over V–Ti/MCM-41 photocatalyst. *Catalysis Today*, *245*, 186–191. https://doi.org/10.1016/j.cattod.2014.06.027

Raillard, C., Héquet, V., Le Cloirec, P., & Legrand, J. (2004). Kinetic study of ketones photocatalytic oxidation in gas phase using TiO 2 -containing paper: effect of water vapor. *Journal of Photochemistry and Photobiology A: Chemistry*, *163*, 425–431. https://doi.org/10.1016/j.jphotochem.2004.01.014

Sakai, H., Kubota, Y., Yamaguchi, K., Fukuoka, H., & Inumaru, K. (2013). Photocatalytic decomposition of 2-propanol and acetone in air by nanocomposites of pre-formed TiO2particles and mesoporous silica. *Journal of Porous Materials*, *20*(4), 693–699. https://doi.org/10.1007/s10934-012-9643-5

Song, H., Li, Y., Lou, Z., Xiao, M., Hu, L., Ye, Z., & Zhu, L. (2015). Synthesis of Fe-doped WO3 nanostructures with high visible-light-driven photocatalytic activities. *Applied Catalysis B: Environmental*, *166–167*, 112–120. https://doi.org/10.1016/j.apcatb.2014.11.020

Verbruggen, S. W., Masschaele, K., Moortgat, E., Korany, T. E., Hauchecorne, B., Martens, J. A., & Lenaerts, S. (2012). Factors driving the activity of commercial titanium dioxide powders towards gas phase photocatalytic oxidation of acetaldehyde. *Catalysis Science & Technology*, *2*(11), 2311-2318. https://doi.org/10.1039/c2cy20123b

Verbruggen, S. W., Ribbens, S., Tytgat, T., Hauchecorne, B., Smits, M., Meynen, V., ... & Lenaerts, S. (2011). The benefit of glass bead supports for efficient gas phase photocatalysis: case study of a commercial and a synthesised photocatalyst. *Chemical engineering journal*, *174*(1), 318-325. https://doi.org/10.1016/j.cej.2011.09.038

Xu, W., & Raftery, D. (2001). In situ solid-state nuclear magnetic resonance studies of acetone photocatalytic oxidation on titanium oxide surfaces. *Journal of Catalysis*, *204*(1), 110–117. https://doi.org/10.1006/jcat.2001.3380